



Executive summary

Development of an improved model for predicting fatigue crack growth in aluminium alloy helicopter airframe components



Problem area

Most of the currently operational helicopter types have been designed according to the safe life philosophy. This implies that principal structural items that are fatigue critical must be retired at a prescribed moment in time (in terms of flight hours or flight cycles), well before the occurrence of fatigue damage is to be expected. In spite of this, in-service fatigue cracks are frequently encountered. In the current practice of 'repair when detected' this leads to unscheduled maintenance and down-time and, therefore, reduced operational availability. To enable the switch to the more desirable practice of 'repair when convenient', tools are needed to assess the severity of in-service fatigue cracks.

Description of work

At NLR a number of activities are being performed that contribute to the development of a so-called operational damage assessment tool. The main objectives are (i) to develop a reliable and practical method for predicting fatigue crack growth in aluminium alloy helicopter airframe components, and (ii) to develop a reliable and practical method for correlating the fatigue loads in helicopter airframe components to the flight conditions and/or flight parameters that are recorded on-board. The scope of the present document is limited to item (i), viz. the development of an improved fatigue crack growth model that is based on the state-of-the-art Strip Yield model as incorporated in the NASGRO and ESACRACK codes.

Report no.

NLR-TP-2007-406

Author(s)

M.J. Bos

Report classification

UNCLASSIFIED

Date

July 2008

Knowledge area(s)

Health Monitoring & Maintenance of Aircraft
Computational Mechanics & Simulation Technology
Helicopter Technology

Descriptor(s)

Fatigue crack growth
Damage tolerance
Helicopters
Strip Yield model

This report is based on a paper presented at the 24th ICAF Symposium in Naples, Italy, 18 May 2007.

Results and conclusions

A research model has been developed which, due to its open and easy architecture, can serve as a platform to test new concepts regarding the constraint behaviour of the material at the crack tip, fatigue crack growth propagation laws, etc. The model has been used to demonstrate that the apparently unique relation between the cyclic crack tip opening displacement and the effective cyclic stress intensity factor exists only under the condition of no-crack-closure. Further research will be conducted

to investigate whether the use of the cyclic crack tip opening displacement as a fatigue crack growth correlating parameter will enhance the capability to predict crack growth under variable amplitude loading.

Applicability

The results of this work contribute to the development of a tool that can be used to assess the severity of in-service fatigue cracks in helicopter airframe components.



NLR-TP-2007-406



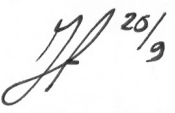
Development of an improved model for predicting fatigue crack growth in aluminium alloy helicopter airframe components

M.J. Bos

This report is based on a paper presented at the 24th ICAF Symposium in Naples, Italy, 18 May 2007.
The contents of this report may be cited on condition that full credit is given to NLR and the author.
This publication has been refereed by the Advisory Committee AEROSPACE VEHICLES.

Customer	Defence Materiel Organisation
Contract number	M/2004004961
Owner	National Aerospace Laboratory NLR
Division	Aerospace Vehicles
Distribution	Unlimited
Classification of title	Unclassified
	July 2008

Approved by:

Author  17/8/07	Reviewer  17/9/07	Managing department  25/9
--	--	--

Summary

The National Aerospace Laboratory NLR in the Netherlands has embarked on the research programme 'HeliDamTol', which aims to improve the capability of assessing the severity of in-service fatigue cracks in helicopter airframes. The present document briefly describes and discusses the programme and the programme status, with particular emphasis on the work involved in the development of an improved Strip Yield model for predicting fatigue crack growth in aluminium alloy helicopter airframe components. This research model has been developed as a Matlab application and due to its open and easy architecture it can also serve as a platform to test new concepts that might arise regarding the constraint behaviour of the material at the crack tip, fatigue crack growth propagation laws, etc. The model has been used to demonstrate that the apparently unique relation between the cyclic crack tip opening displacement and the effective cyclic stress intensity factor exists only under the condition of no-crack-closure. Further research will be conducted to investigate whether the use of the cyclic crack tip opening displacement as a fatigue crack growth correlating parameter will enhance the capability to predict crack growth under variable amplitude loading.

Contents

1 Introduction	7
2 HeliDamTol	7
3 Fatigue crack growth model	8
4 Conclusions	24
References	25
Appendix A - Crack tip stress/displacement behaviour (graphs)	29

Abbreviations

a	(Half) crack size.
a_{eff}	Effective (half) crack size.
CA	Constant Amplitude.
cod(i)	Crack Opening Displacement at strip yield element i.
CTOD	Crack Tip Opening Displacement.
da/dN	Fatigue crack growth rate in units of length per cycle.
D_p	Plastic zone size.
DT	Damage Tolerance.
E	Elastic modulus.
FAA	Federal Aviation Administration.
FEA	Finite Element Analysis.
K	Crack tip stress intensity factor.
K_{max}	Maximum crack tip stress intensity factor in load cycle.
K_{min}	Minimum crack tip stress intensity factor in load cycle.
K_{op}	Crack tip stress intensity factor above which the crack is open.
LEFM	Linear Elastic Fracture Mechanics.
NLR	Nationaal Lucht- en Ruimtevaart laboratorium (National Aerospace Laboratory).
PPZ	Primary Plastic Zone.
R	Cyclic stress ratio.
sl(i)	Stretch Left on crack flank at strip yield element i.
v(i)	Elastic displacement of crack flank at strip yield element i.
VA	Variable Amplitude.
w(i)	Width of a strip yield element i.
x(i)	Location of strip yield element i.
α	Constraint factor, to be applied to the uni-axial yield limit to simulate the three-dimensional stress state in the plastic zone ahead and in the wake of the crack tip.
α_c, α_t	Constraint factor under compressive loading and tensile loading respectively.
ΔCTOD	Cyclic Crack Tip Opening Displacement.
ΔK	Cyclic stress intensity range $K_{\text{max}} - K_{\text{min}}$.
ΔK_{eff}	Effective cyclic stress intensity range $K_{\text{max}} - K_{\text{op}}$.
ΔK_1	Threshold stress intensity range for constant amplitude loading at R approaching 1.
$\sigma(i)$	Stress that acts on strip yield element i.
σ_r	Applied remote stress.
σ_{yld}	Uni-axial yield stress.
σ_0	Flow stress.



This page is intentionally left blank.

1 Introduction

Encouraged by the FAA [1], the helicopter airframe manufacturers in the USA and Europe are slowly moving towards the Damage Tolerance (DT) design approach. At the same time, military operators of aging helicopter fleets are increasingly confronted with fatigue related maintenance issues and the need for structural life extension programmes. The application of the DT approach could significantly contribute to the resolution of these issues, in terms of weapon system availability (Can a helicopter with a just-detected crack be flown safely until scheduled maintenance? Which flight conditions should be avoided?) and economy (How much longer can the fleet be safely operated beyond the design safe life?).

However, owing to the particular loading conditions encountered by many helicopter components, the implementation of the DT approach is more difficult than for fixed-wing aircraft. In particular, recent research has shown that currently available models do not accurately predict fatigue crack growth under helicopter spectrum loading. Although these models are reasonably successful for DT evaluations of fixed-wing aircraft, they show large scatter and tend to be unconservative when predicting crack growth lives in helicopter components [2-4]. Also various authors have suggested that (i) insufficient and even inappropriate crack growth data are used for the near-threshold ΔK vs. da/dN regime that is most important for the high-cycle (vibratory) fatigue that occurs in helicopters [5], and (ii) load interaction effects for the special characteristics of helicopter spectra (many high R-ratio cycles, few underloads) are not properly accounted for [6]. These problems must be studied thoroughly, since any DT-based design and maintenance concept relies heavily on good crack growth predictions, and crack growth rates in helicopter components can be high owing to high overall stress levels and the high frequencies pertaining to vibratory fatigue.

2 HeliDamTol

In the light of the foregoing problems and considerations, the National Aerospace Laboratory NLR in the Netherlands has embarked on the research programme 'HeliDamTol'. The main objectives of this programme are (i) to develop a reliable and practical method for predicting fatigue crack growth in aluminium alloy helicopter airframe components, and (ii) to develop a reliable and practical method for correlating the fatigue loads in helicopter airframe components to the flight conditions and/or flight parameters that are recorded on-board. To date, most of the activities performed are related to improving a state-of-the-art crack growth model, namely the Strip Yield

model that is incorporated in the NASGRO and ESACRACK codes. These activities include:

- Finite Element Analysis (FEA) of the plastic zone around the crack tip;
- Experimental work to determine basic material properties of two selected aluminium alloys (da/dN vs. ΔK , fatigue crack growth threshold values, monotonic and cyclic stress/strain behaviour);
- Experiments to study load interaction effects under simplified helicopter spectrum loading (including crack closure measurements and fractographic analysis); and
- Experiments using realistic helicopter spectrum loading to obtain benchmarks for model validation.

The study is limited to conventional aluminium alloys that are used in the airframes of helicopter types that are currently flown or are about to be flown by the Air Command of the Royal Netherlands Armed Forces, viz. 7050-T7451 (CH-47D) and 7075-T7351 (NH90). The stress spectra will reflect the typical usage of this operator and these helicopter types and have been/will be obtained from actual flight measurements. To this end, a CH-47D helicopter has been equipped with a data acquisition unit and a recorder which stores the digital signals from the data bus plus the analogue signals from nine strain gauges in the aft fuselage.

The scope of the present document is limited to the development of the improved variable constraint-loss Strip Yield model.

3 Fatigue crack growth model

Fatigue crack growth predictions are usually based on the results from experiments in which a fatigue crack is grown under constant amplitude (CA) loading until failure of the test specimen. In general a number of experiments are conducted to cover the whole range of expected stress ratios, R . Additionally, specific experiments may be done to establish the appropriate fatigue crack growth threshold values. Assuming a unique relation between the fatigue crack growth rate, da/dN , and a limited number of characteristic parameters such as the crack tip stress intensity range, ΔK , and the stress ratio (though environmental factors like temperature and humidity may also be significant) the experimental data can be used – in theory – to analyse the more general condition of fatigue crack growth under variable amplitude (VA) loading. In practice, however, interaction of the load cycles of different amplitudes and mean levels will cause either crack growth retardation or crack growth acceleration, relative to the crack growth as expected from a linear summation of the experimentally established crack growth rates for the individual CA load cycles that constitute the VA load spectrum.

Various models are available to account for these load interaction effects. Many of them are based on the premise that load interaction is plasticity-induced. The application of a load on a structural component containing a crack results in formation of a plastic zone ahead of the crack tip. The size of this plastic zone is proportional to the square of the crack tip stress intensity factor, K , and therefore strongly depends on the magnitude of the applied load.

Some of the older models, such as those due to Wheeler [7] and Willenborg [8,9], treat load interaction as an effect that occurs due to the modified residual stress distribution in the material ahead of the crack tip. These models are based on the assumption that the plastic zone that is produced by an overload will retard subsequent crack growth by reduction of the effective crack tip stress intensity or stress intensity ratio, until the crack has grown through this plastic zone. Although reasonably successful and widely used (especially the Willenborg model, albeit in modified form), these models cannot cope with more intricate interaction effects such as delayed retardation, which has often been observed. Moreover, the model “tuning” needed to correlate predictions to experimental data tends to depend on load level, spectrum shape and the exact sequence of loads within a spectrum [10].

There are other, more recent, models lacking specificity about the underlying mechanism of load interaction. The K_{pr} -model [3], for instance, is empirical; the model parameters needed to describe the effects of load interaction are derived from a set of dedicated well-specified experiments under VA loading, additional to the CA crack growth tests that are needed to characterise the basic fatigue crack growth behaviour.

Strip Yield model

A model with much more potential (but also much greater complexity) is the Strip Yield model, which has already been implemented in various different computer programs, e.g. FASTRAN [11], NASGRO [12] and ESACRACK [13]. The Strip Yield model is based on the concept of crack closure that was already introduced in the early 1970s by Elber [14]. He argued that if the crack grows through the plastic zone ahead of its tip, it leaves behind a wake of residual plastic deformations on the crack flanks. These deformations will cause the crack to close prematurely upon unloading, thereby reducing the effective (i.e. crack driving) stress range and thus the effective crack tip stress intensity range ΔK_{eff} , which is usually defined as:

$$\Delta K_{eff} = K_{max} - K_{min,eff} = K_{max} - K_{op} \quad (1)$$

where K_{\max} is the maximum cyclic crack tip stress intensity and K_{op} is the minimum stress intensity factor at which the crack is still open when decreasing the applied load level or the maximum stress intensity factor at which the crack is still closed when increasing the load (these stress intensity factors are practically the same).

In the development of Eqn. 1 it was implicitly assumed that the stress field around the crack tip is governed by the presence of the so-called singularity. Any effect due to the compressive residual stresses in the plastic zone due to previous loads will be negated once the crack opens under the applied remote loading. Whereas in the Willenborg model *both* the minimum and the maximum cyclic stress intensity factors are adjusted to establish the effect of plasticity induced load interaction, in the Strip Yield model (and also in the K_{pr} -model) this adjustment is only done for the minimum value, in line with the concept of crack closure. It has been shown by numerous authors that crack closure can explain the stress ratio effect on fatigue crack growth by collapsing the experimentally determined crack growth curves for different R values to a single curve that depends only on ΔK_{eff} .

The characteristic of the Strip Yield model that distinguishes it from other closure-based models is that it explicitly keeps track of the plastic deformations that are left in the wake of the growing crack. The plastic deformations in the material ahead of the crack tip (which eventually will end up in the wake) are characterised by the plastic zone size, D_p , and the crack tip opening displacement, CTOD. To estimate the values of these parameters, Dugdale [15] proposed modelling the plastic zone as a virtual extension of the actual crack – see figure 1 – while assuming that plasticity is confined to an infinitesimally thin strip along the crack, and with ideal plastic behaviour (i.e. no deformation when loaded in the elastic range of stresses and indeterminate deformation at \pm the yield stress, σ_{yld}).

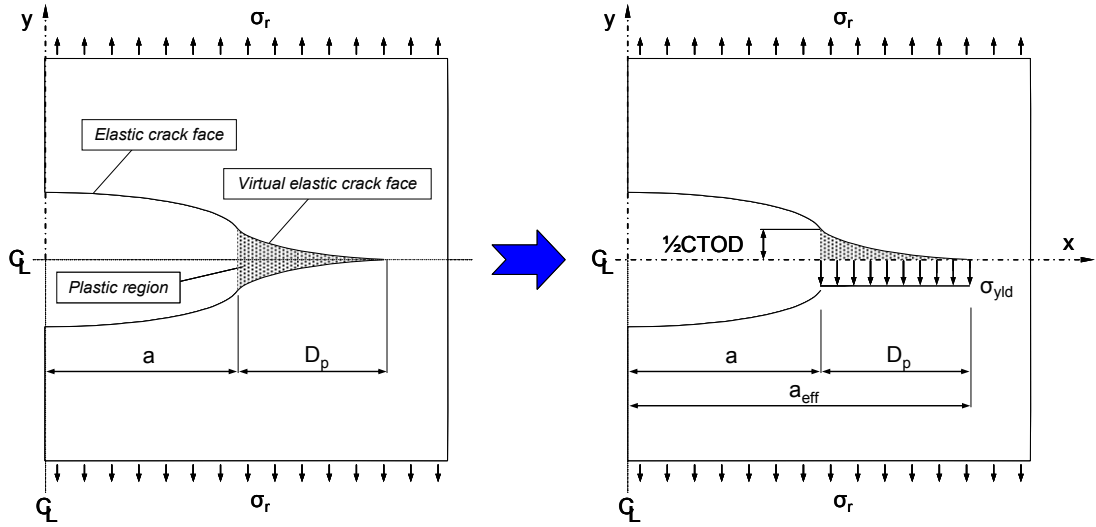


Figure 1 - Fictitious crack in the Dugdale model.

The resulting system can be described with the appropriate linear elastic fracture mechanics (LEFM) equations. By loading the flanks of the virtual part of the crack by a uniform tensile stress that is equal to the yield stress, and equating the sum of the virtual crack tip stress intensity factors due to this loading and the remote loading to zero (thereby removing the singularity), Dugdale found for the CTOD and the monotonic primary plastic zone (PPZ, formed in ‘virgin’ material):

$$CTOD = \frac{8\sigma_{yld}a}{\pi E} \ln \left(\sec \frac{\pi\sigma_r}{2\sigma_{yld}} \right) \quad (2)$$

and

$$a_{eff} = a + D_p = \frac{a}{\sin \frac{1}{2} \pi \left(1 - \frac{\sigma_r}{\sigma_{yld}} \right)} \quad (3)$$

where a is the actual crack size (or half crack size in the case of a centre crack), a_{eff} is the effective crack size, σ_r is the applied remote stress and σ_{yld} is the yield stress. These equations are valid for an infinite sheet with a centre through-crack. Correction factors for finite width are available for a limited number of geometries, see for instance [16]. Using a series expansion, the equations for the CTOD and the plastic zone size are usually approximated as:

$$CTOD = \frac{K^2}{E\sigma_{yld}} \quad (4)$$

and

$$D_p = \frac{\pi}{8} \left(\frac{K}{\sigma_{yld}} \right)^2 \quad (5)$$

These approximate equations are valid only for $\sigma_r \ll \sigma_{yld}$. This is illustrated in figure 2.

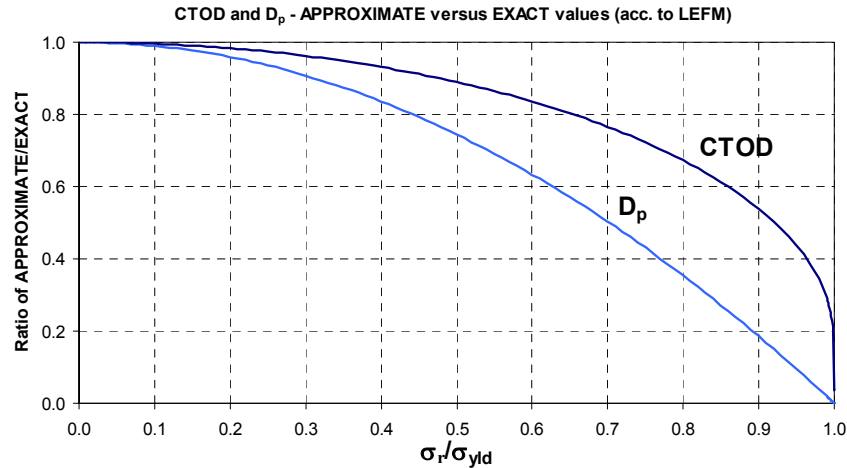


Figure 2 - Comparison of the approximate and exact values for the crack tip opening displacement and the plastic zone size.

Note that Eqns. 2-5 are based on the assumption of a uniformly distributed load in the PPZ that is equal to the uniaxial monotonic yield limit. In practice the yield limit may be significantly greater owing to in-plane and out-of plane constraint effects that give rise to a complicated three-dimensional stress state at the crack tip. This state is governed by the ratio of plastic zone size and plate thickness. Ratios of less than about 0.1 are associated with the condition of plane strain, larger ratios of about 1.5 lead to plane stress. The yield stress in Eqns. 2-5 is therefore usually replaced by the term ' $\alpha\sigma_0$ ', where α is the so-called constraint factor (usually in the range of 1.0 for plane stress to 3.0 for plane strain) and σ_0 is the flow stress, which is taken as the average of the yield stress and the ultimate stress as a first order approximation of strain hardening. Moreover, the constraint factor for the PPZ tends to decay quadratically with the distance from the crack tip [17].

The description of the constraint behaviour requires a model in itself. For example, distinction needs to be made between whether the plastic zone under consideration is formed in tension (tensile constraint factor α_t) or in compression (reversed loading, α_c); and, if in tension¹, whether the zone is primary (formed by an overload) or secondary

¹ A primary plastic zone in compression would imply large scale yielding, which is not relevant within the present context.

(after load reversal). Various models are available, the main difference being whether the constraint is spatially constant over the plastic zone, like the one due to Newman [11,12], or whether it is variable as in the model of De Koning [17]. Recent studies have indicated that the latter type of model allows better correlation with local compliance measurements [18,19]. However, the increased number of model parameters make a variable constraint model more difficult to use.

As already stated, the Strip Yield model explicitly keeps track of the plastic deformations that are left in the wake of the growing crack. To achieve this, the system of figure 1 is discretised into N small strip yield elements, with each element i having a specific width $w(i)$, an acting uniform stress $\sigma(i)$, a residual plastic stretch $sl(i)$ that is left after unloading², an elastic displacement perpendicular to the crack $v(i)$, and a crack opening displacement $cod(i)$. This discretisation is depicted in figure 3. For each element the $v(i)$ is equal to the sum of $sl(i)$ and $cod(i)$. For the elements in the PPZ $cod(i)$ equals zero and $\sigma(i)$ is limited by $-\alpha\sigma_0$ and $+\alpha\sigma_0$. The element stresses in the wake of the crack tip are limited by $-\alpha\sigma_0$ and 0.

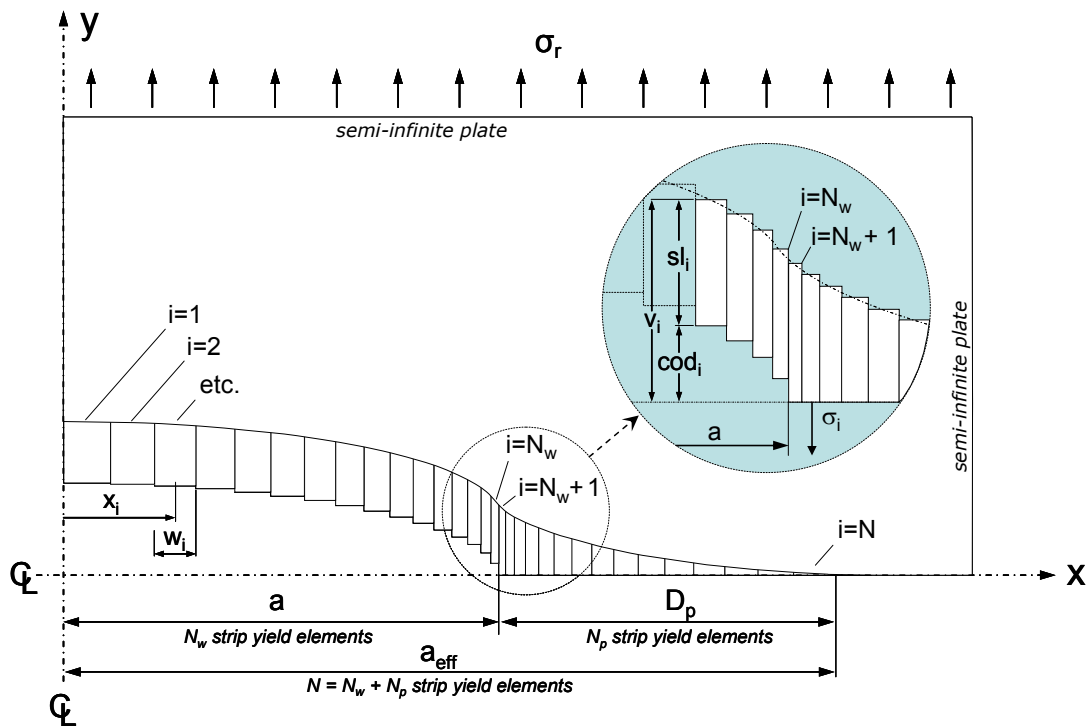


Figure 3 - Discretised Strip Yield model.

² Note that the plastic strain cannot be derived directly from this stretch, because the initial stretch (i.e. length) of the elements is zero.

The system of figure 3 can be solved with the following LEFM equations:

$$v(i) = GV(i) \cdot \sigma_r - GM(i, j) \cdot \sigma(j) \quad (6)$$

where the influence vector GV and influence matrix GM are given by:

$$GV(i) = \frac{2}{E} \sqrt{a_{eff}^2 - x(i)^2} \quad (7)$$

and

$$GM(i, j) = \frac{2}{\pi E} \left[b_2(j) \ln \left| \frac{\sqrt{a_{eff}^2 - b_2(j)^2} + \sqrt{a_{eff}^2 - x(i)^2}}{\sqrt{a_{eff}^2 - b_2(j)^2} - \sqrt{a_{eff}^2 - x(i)^2}} \right| - b_1(j) \ln \left| \frac{\sqrt{a_{eff}^2 - b_1(j)^2} + \sqrt{a_{eff}^2 - x(i)^2}}{\sqrt{a_{eff}^2 - b_1(j)^2} - \sqrt{a_{eff}^2 - x(i)^2}} \right| - \right. \\ \left. x(i) \left(\ln \left| \frac{x(i)\sqrt{a_{eff}^2 - b_2(j)^2} + b_2(j)\sqrt{a_{eff}^2 - x(i)^2}}{x(i)\sqrt{a_{eff}^2 - b_2(j)^2} - b_2(j)\sqrt{a_{eff}^2 - x(i)^2}} \right| - \ln \left| \frac{x(i)\sqrt{a_{eff}^2 - b_1(j)^2} + b_1(j)\sqrt{a_{eff}^2 - x(i)^2}}{x(i)\sqrt{a_{eff}^2 - b_1(j)^2} - b_1(j)\sqrt{a_{eff}^2 - x(i)^2}} \right| \right) - \right. \\ \left. 2\sqrt{a_{eff}^2 - x(i)^2} \left(\cos^{-1} \left(\frac{b_2(j)}{a_{eff}} \right) - \cos^{-1} \left(\frac{b_1(j)}{a_{eff}} \right) \right) \right] \quad (8)$$

In the above equations $b_1(j)$ and $b_2(j)$ are the x-coordinates of the left and right boundaries of element j and E is the elastic modulus. Alternatively, a simpler but less accurate description of GM is given by the following equation, which is the LEFM solution for a concentrated force at the centre of element j:

$$GM(i, j) = \frac{2w(j)}{\pi E} \ln \left| \frac{\sqrt{a_{eff}^2 - x(j)^2} + \sqrt{a_{eff}^2 - x(i)^2}}{\sqrt{a_{eff}^2 - x(j)^2} - \sqrt{a_{eff}^2 - x(i)^2}} \right| \quad (9)$$

In vector notation, Eqn. 6 can be rewritten as:

$$\begin{pmatrix} \bar{v}_k \\ \bar{v}_u \end{pmatrix} = \begin{pmatrix} \overline{GV}_k \\ \overline{GV}_u \end{pmatrix} \cdot \sigma_r - \begin{pmatrix} \overline{GM}_{ku} & \overline{GM}_{kk} \\ \overline{GM}_{uu} & \overline{GM}_{uk} \end{pmatrix} \cdot \begin{pmatrix} \bar{\sigma}_u \\ \bar{\sigma}_k \end{pmatrix} \quad (10)$$

where a single bar denotes a column vector and a double bar indicates a matrix. In the above equation \bar{v}_k is the vector of known displacements (in the PPZ, for elements that do not yield; and in the wake, if the element stress is compressive and does not exceed the yield stress), \bar{v}_u is the vector of unknown displacements, $\bar{\sigma}_u$ is the vector of

unknown element stresses (for the elements with a known displacement) and $\bar{\sigma}_k$ is the vector of known element stresses (for elements that either yield or, in the wake, are not in contact).

Since knowing the displacement is equivalent to not knowing the element stress, the submatrix $\overline{\overline{GM}}_{ku}$ is square and can be inverted. This leads to the following set of equations for the unknown parameters:

$$\bar{\sigma}_u = \overline{\overline{GM}}_{ku}^{-1} \cdot \left(\overline{\overline{GV}}_k \cdot \sigma_r - \overline{\overline{GM}}_{kk} \cdot \bar{\sigma}_k - \bar{v}_k \right) \quad (11a)$$

and

$$\bar{v}_u = \overline{\overline{GV}}_u \cdot \sigma_r - \overline{\overline{GM}}_{uu} \cdot \bar{\sigma}_u - \overline{\overline{GM}}_{uk} \cdot \bar{\sigma}_k \quad (11b)$$

The remote stress is supplied to the model as a sequence of peaks and valleys. Upon application of a load step, Eqn. 11 needs to be solved iteratively, since it is not known *a priori* to which part of the equation each element belongs. In each iteration loop it is therefore checked whether the constraints on $\text{cod}(i)$ and $\sigma(i)$ are violated and corrective actions are taken if necessary (while making sure that the solution converges!). The influence vector $\overline{\overline{GV}}$ and influence matrix $\overline{\overline{GM}}$ need to be updated only when the crack is (incrementally) grown and remeshing of the strip yield elements has been performed. The crack is grown according to the effective stress intensity factor range ΔK_{eff} (or any other crack growth correlating parameter) as computed with the model and according to an appropriate crack growth law that has to be specified. We note here that the crack growth law needs to be compatible with the applied constraint model, in order to avoid erroneous results [21]

The model described so far has already been implemented in various different computer programs. Within the context of the HeliDamTol programme, however, there is a need for an easy-to-use and (especially) easy-to-adjust crack growth analysis tool serving as a testbed for the various submodels and other concepts that might arise. Since the Strip Yield model is considered to be the most versatile and potentially accurate of all load interaction models, it was selected for implementation in a Matlab-based test environment.

Using the extensive functionality that Matlab offers, a flexible and adaptive tool has been developed that currently incorporates seven different constant- or variable-constraint models. Care has been taken to vectorize the required matrix operations as much as possible, in order to minimize the computational time. In principle this Matlab implementation of the Strip Yield model is meant for research purposes only. If

computational speed becomes an issue (i.e. if production software is needed), the developed (sub)models should be incorporated in computationally more efficient, but implementation-wise less flexible, software such as NASGRO.

Since one of the aims of HeliDamTol is to improve the predictive capability of crack growth under helicopter spectrum loading, a new meshing routine has been devised that adjusts the sizes of the strip yield elements such that the model can capture reversed yielding under the smallest stress range occurring in the input load sequence. Stress ranges that will never lead to exceeding the fatigue crack growth threshold are filtered out beforehand, based on the criterion that the ratio of the remaining minimum stress range to the maximum peak stress should be greater than the ratio of the intrinsic fatigue crack growth threshold ΔK_1 (which is the value at a stress ratio that approaches one) to the critical stress intensity factor K_c . The calculation of the minimum element width, for the element at the crack tip, is obtained from the following modification of Eqn. 5:

$$w_{tip} = \frac{\pi}{8} \left(\frac{\max(\Delta K_1, \Delta K_{min})}{2\alpha_t \sigma_{yld}} \right)^2 \quad (12)$$

where ΔK_{min} is the stress intensity factor range associated with the remaining minimum spectrum stress range and α_t is the tensile constraint factor at the crack tip.

New approach

The main novelty in the Matlab implementation of the Strip Yield model, however, is related to the crack propagation law. In the recent past various authors have expressed the belief that a crack growth law based on ΔK_{eff} alone may not be adequate, and that plasticity induced closure is not the only explanation for load interaction effects [22,23]. For many cases this may be true. For example, in materials such as Al-Li alloys, roughness-induced closure under VA loading may play a significant role [24]; and for specific materials and specific environmental conditions, oxide layers that are formed on the crack surface may also raise the minimum effective crack tip stress intensity [25]. Additionally, microstructural effects may cause the tip of a growing crack to be irregular (tortuosity), thereby affecting the crack tip stress intensity factors.

The Strip Yield model will not be able to cope directly with these types of effects. However, for many practical engineering problems the concept of crack closure has proven to be a fundamentally sound notion, with much support from experimental data and finite element results. Even so, there is still potential to improve the crack propagation law. In their 1997 paper Guo and his co-workers postulated that the fatigue

crack growth rate is uniquely determined by the cyclic crack tip opening displacement, $\Delta CTOD$ [16]. They based this proposition on the physical argument that crack growth occurs predominantly by the mechanism of blunting and resharping. Additionally they observed by comparison of Eqns. 4 and 5 that the crack tip plastic zone size shows a stronger sensitivity to the yield stress (and therefore to the constraint factor α) than the CTOD does. Thus it may be more appropriate to consider $\Delta CTOD$ as a fatigue crack growth correlating parameter. This is confirmed by Noroozi, Glinka and Lambert [26] who convincingly show that crack growth can be expressed and analysed in terms of local crack tip stress-strain response. Their elastic-plastic strip yield-like analysis, however, is sensitive to the assumed value for the crack tip radius. From a practical point of view this is undesirable.

The approach followed here is more pragmatic in that it uses existing experimental fatigue crack growth data in the classical form of da/dN versus ΔK , for a range of R values. These data are fed into the Strip Yield model, which in the so-called ‘calibration mode’ is used to simulate crack growth under CA loading. Traditionally the crack growth rate would be determined on the basis of the computed values of ΔK_{eff} . In the calibration mode, however, the Strip Yield model simply uses the applied ΔK (as computed directly from the CA load sequence and the momentary crack size) and the experimental da/dN versus ΔK data. At each load step the calculated value for the cyclic crack tip opening displacement is paired with the value for da/dN , and the results are used to construct either a look-up table or a regression curve with da/dN versus $\Delta CTOD$ and $CTOD_{max}$ values.

This simple and straightforward process is depicted in figure 4.

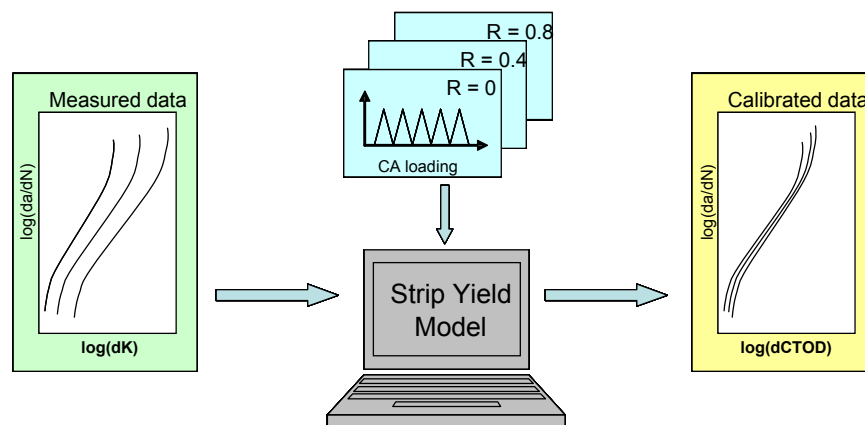


Figure 4 - Calibration of the material data.

Correlation on the basis of $\Delta CTOD$ alone does not necessarily give satisfactory results, depending on the selected constraint model. This seems to confirm the position of Sadananda [23] and many others, who state that fatigue crack propagation is inherently also driven by K_{max} (and therefore $CTOD_{max}$) instead of by ΔK_{eff} alone. Similar to the two-parameter model proposed by Kujawski and others [22], the following function is therefore used to correlate da/dN :

$$da/dN = C \left(\Delta CTOD^m \cdot CTOD_{max}^{(1-m)} \right)^n \frac{\left(1 - \frac{\Delta CTOD_{th}}{\Delta CTOD} \right)^p}{\left(1 - \frac{CTOD_{max}}{CTOD_c} \right)^q} \quad (13)$$

Where $\Delta CTOD_{th}$ is the threshold CTOD range below which no crack growth will occur, and $CTOD_c$ is the critical value at the onset of failure. The parameter m in Eqn. 13 serves to distribute the crack propagation mechanism between strictly cyclic ($m=1$), strictly static ($m=0$) and anything in between ($0 < m < 1$).

The CTOD is calculated at the *actual* crack tip (i.e. not at the centre of the first element ahead of the tip). For this purpose Eqn. 8 is used in conjunction with the calculated element stresses except for the elements adjacent to the crack tip; for these elements Eqn. 8 contains a singularity and is therefore replaced by Eqn. 9. Note that the model computes the value for the parameter ‘sl’ – see figure 3 – so the values for CTOD as computed by the present model are actually 50% of those calculated with Eqn. 2.

An example of the results of the correlation process is given in figure 5. For the ‘experimental’ da/dN versus ΔK input data, use has been made of the NASGRO fatigue crack growth equation [12] in conjunction with the material parameters for 7075-T7351 as provided by NASGRO version 4.12. The data have been fitted for both the variable constraint model of De Koning (figure 5a) and the constant constraint model of Newman, with a crack tip tensile constraint value α_t of 2.0 (plane strain) and a compressive tip constraint value α_c of 1.0 (figure 5b). The plate thickness has been set to 0.01 m to postpone the activation of constraint loss to higher values of ΔK_{eff} .

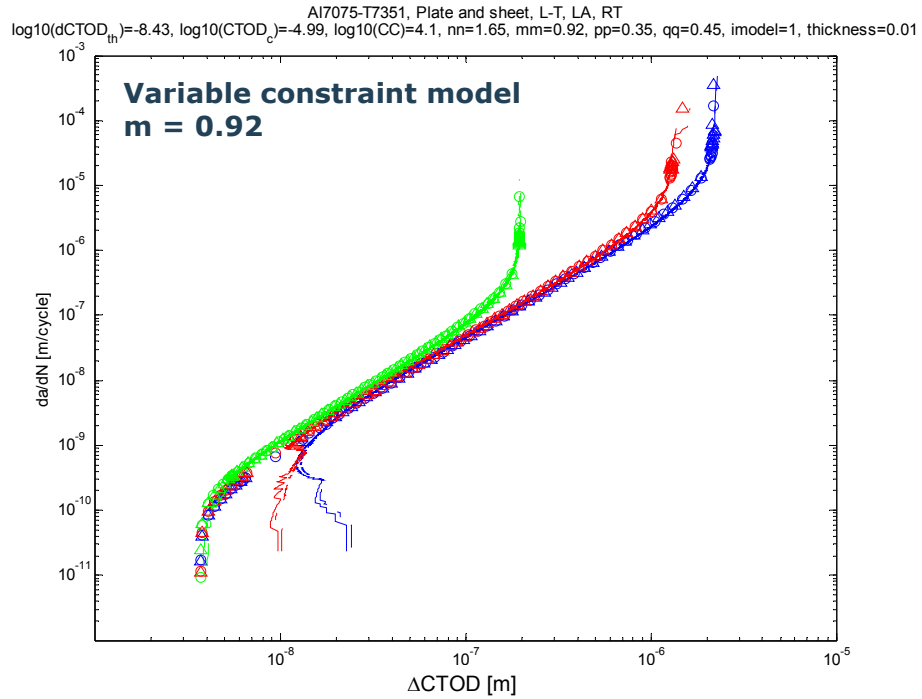


Figure 5a - Calibration results for 7075-T7351 in conjunction with the variable constraint model of De Koning (blue: $R=0$, red: $R=0.4$, green: $R=0.8$).

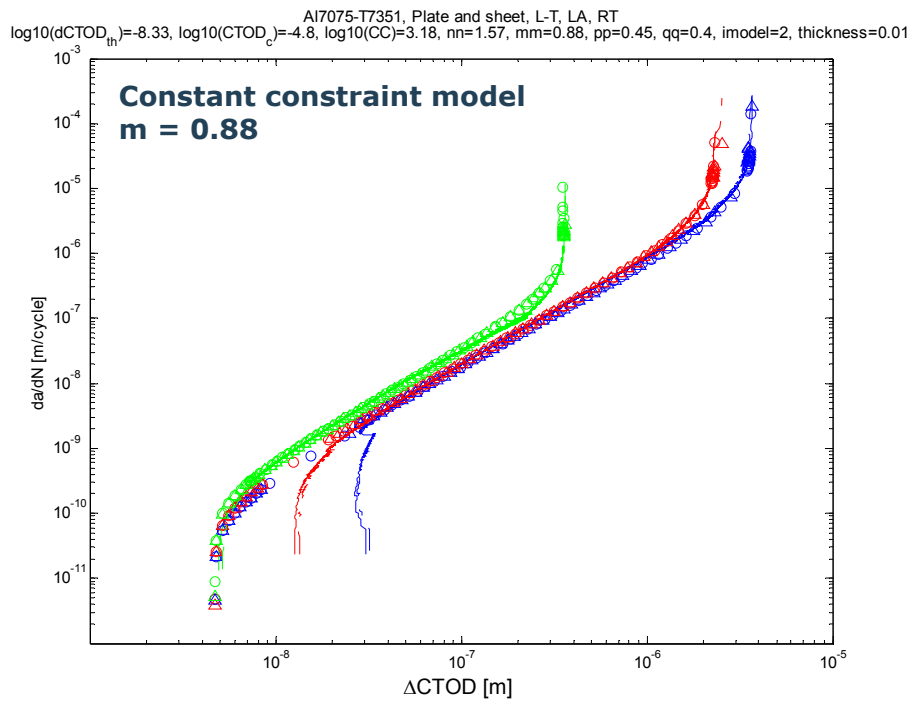


Figure 5b - Calibration results for 7075-T7351 in conjunction with the constant constraint model of Newman (blue: $R=0$, red: $R=0.4$, green: $R=0.8$).

In figure 5 the solid lines are the Strip Yield simulation results and the symbols denote the fitted results as calculated with Eqn. 13. The erratic parts of the R=0 and R=0.4 curves near the threshold are caused by the fact that there is no residual plastic deformation present on the flanks of the initial crack in the Strip Yield model. The associated crack growth rate is calculated with the NASGRO equation however, which implicitly contains the effect of closure and therefore is too slow. Only after some crack growth do the R=0 and R=0.4 curves attain their stabilised positions. The fit for the R=0.8 data in figure 5b is conservative in the higher da/dN range, where in the Strip Yield model the constraint-loss option has been activated (i.e. the transition to the plane stress state has been reached).

Figures 5a and 5b look similar. They are not identical, however. Note the different fit values for parameters $\Delta CTOD_{th}$, $CTOD_c$ and m (in the header of the graphs). Apparently the correlation between da/dN and $\Delta CTOD$ depends on the selected constraint model.

In principle the constraint model has to be calibrated, or “tuned”, in order to optimize its predictive capability, no matter which constraint model is adopted (spatially variable or spatially constant constraint model). Tuning in this respect means the determination of the appropriate crack tip values for the constraint factors α_t and α_c , by means of trial and error. Usually this is done according to the logic that the fatigue crack growth curves for different R values should collapse to a single curve when plotted against ΔK_{eff} , and that the results of some specific fatigue crack growth experiments under VA loading should be simulated correctly. If the premise of a unique relationship between da/dN and ΔK_{eff} is abandoned, however, the fundamental question arises what other tuning strategy should be followed (if any). An attractive possibility is to consider the adopted constraint model as physically correct and to use the parameter m in Eqn. 13 for tuning. After all, the definition of the constraint model is based (or, at least: should be based) on the results of finite element analyses and other physical considerations, whereas this is much more difficult for the establishment of the relation between da/dN and $\Delta CTOD$ or ΔK_{eff} or any other characteristic parameter. This problem needs to be studied in more detail.

The calibration results of figure 5 seem to suggest that there is a unique relation between ΔK_{eff} and $\Delta CTOD$ (apart from the relatively small $CTOD_{max}$ effect, depending on the applied constraint model). This is in line with Eqn. 4, which according to Guo [16] can be modified as follows:

$$\Delta CTOD = \frac{\Delta K_{eff}^2}{E(\alpha_t + \alpha_c)\sigma_0} \quad (14)$$

However, this equation is only valid under the conditions for which it has been derived, viz. a remote stress that is well below the yield stress, a uniformly distributed stress distribution in the plastic zone ahead of the crack tip, and zero loading on the crack flanks. Assuming that the remote stress indeed remains well below the yield stress, this situation remains true as long as the crack remains stationary and does not grow into the plastic zone ahead of its tip. Once it does, the situation drastically alters and Eqn. 14 becomes invalid, except for higher R values for which closure is absent. The apparent uniqueness of the relation between ΔK_{eff} and ΔCTOD in figure 5 therefore holds only for crack growth under CA loading (and, as said, is only apparent and depends on R), and disappears under VA loading.

This is illustrated by the following example. It pertains to the situation that a 0.01 m centre crack with a fully developed (though artificially defined) plastic wake is cycled according to the following remote stress sequence, with a constant maximum value of 100 MPa and a minimum value that increases from 40 MPa to 90 MPa, with steps of 5 MPa per cycle:

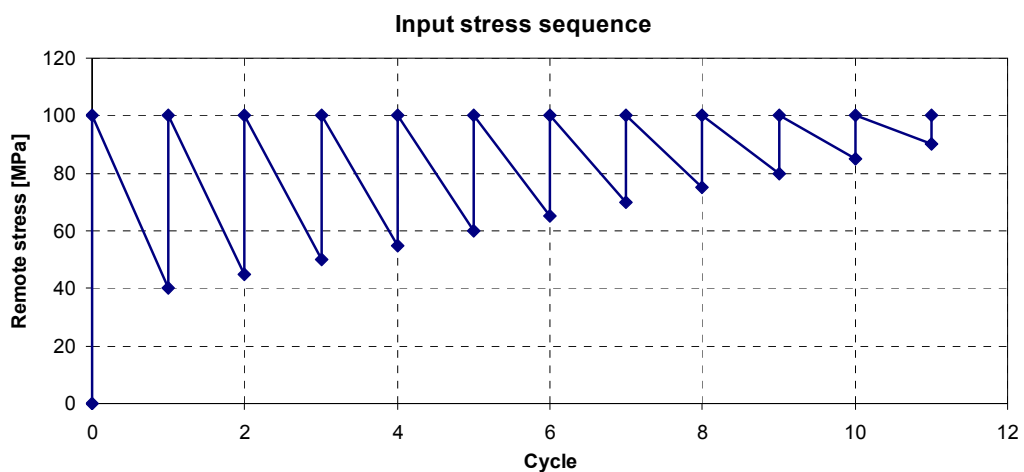


Figure 6 – Input remote stress sequence.

For this example a very fine grid has been used with 100 elements in the PPZ and 300 elements in the wake. The constant constraint model of Newman has been applied. The resulting local stress/displacement behaviour is shown graphically for the remote stress cycles 1, 5 and 9 in Appendix A, figures A.1 to/incl. A.3.

The calculated relation between ΔK_{eff}^2 and $\Delta CTOD$ is shown in figure 7. In figure 8 the normalised value for $\Delta CTOD$ is plotted against the cycle number, where the normalised $\Delta CTOD$ is defined as:

$$Normalised \Delta CTOD = \Delta CTOD \cdot \frac{2E(\alpha_t + \alpha_c)\sigma_0}{\Delta K_{eff}^2} \tag{15}$$

and α_t and α_c are the tensile and compressive constraint factors respectively. The factor 2 in Eqn. 15 has been introduced to account for the fact that the present Strip Yield model equates CTOD to sl at the crack tip – see figure 3.

The results presented in figures 7 and 8 clearly indicate the non-linearity of the relation between $\Delta CTOD$ and ΔK_{eff} . Apparently, Eqn. 14 is only valid, i.e. the normalised $\Delta CTOD$ equals 1, as long as crack closure does not occur (cycles 6 and up). For the cycles for which crack closure does play a role (cycles 5 and below), the relation between $\Delta CTOD$ and ΔK_{eff} is not linear anymore.

Note that the small upturning of the curve during cycles 9 to 11 in figure 8 is caused by numerical inaccuracies that occur for small cyclic CTOD ranges. This underscores the need for a very fine grid in the crack tip area in order to achieve the required accuracy.

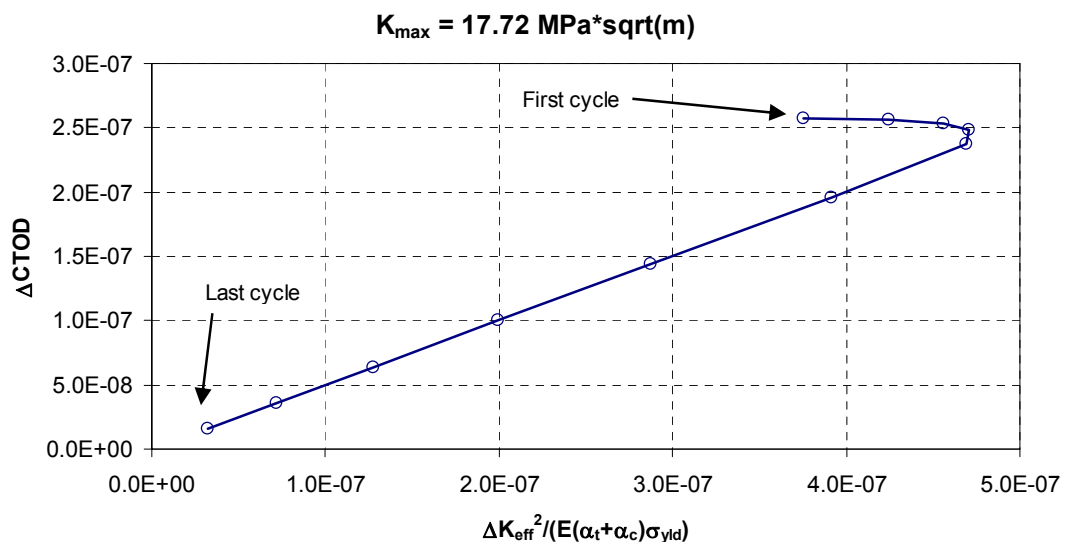


Figure 7 – The relation between ΔK_{eff}^2 and $\Delta CTOD$ for the example remote stress sequence and a fully developed (artificial) plastic wake; crack size = 0.01 m.

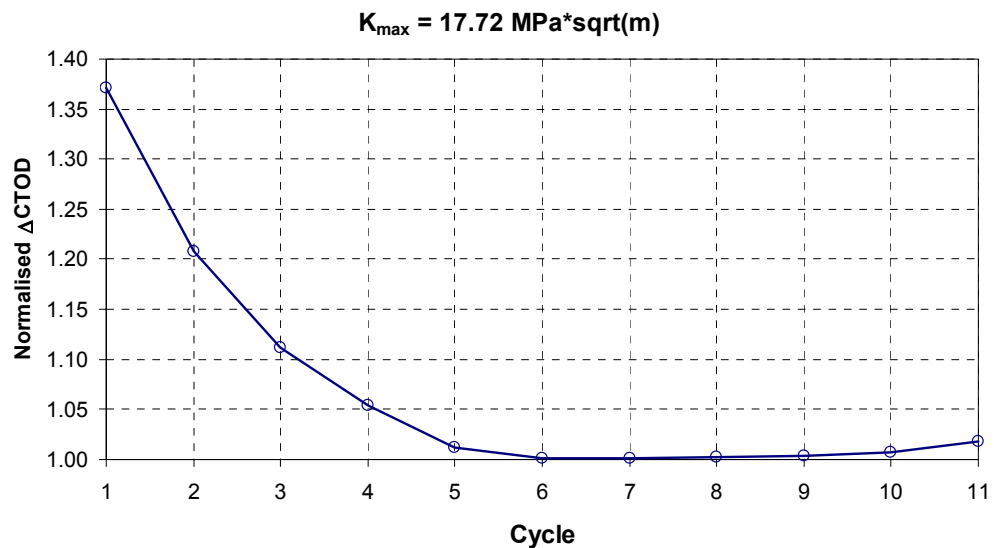


Figure 8 – The normalised ΔCTOD for the example remote stress sequence and a fully developed (artificial) plastic wake; crack size = 0.01 m.

Figure 7 shows a peculiar feature. With decreasing cyclic stress range, which for this example means an increasing K_{\min} , the value for ΔK_{eff} initially *increases*. Only from cycle 4 on does the value for ΔK_{eff} start to decrease. This peculiar feature is caused by the fact that for the particular plastic wake assumed in the example (i.e. linearly decreasing s_l with distance from crack tip), the elements just behind the tip do not close anymore when the ΔK_{eff} starts to decrease. This is illustrated by figure A.2 and is, according to Noroozi, Glinka and Lambert [26], in fact quite normal. During the downward part of a load cycle, the first contact will be made by elements further down the wake and crack tip closure does not take place. Instead, the lever-like situation illustrated by figure 9 will occur, and the unloading of the material further down the wake will effectively increase the crack tip stress intensity. This process is highly non-linear and the CTOD apparently still decreases, albeit with a reduced rate. This again underscores the fact that there is not a unique relation between the CTOD and the crack tip stress intensity factor, or between the cyclic CTOD and the effective cyclic stress intensity factor.

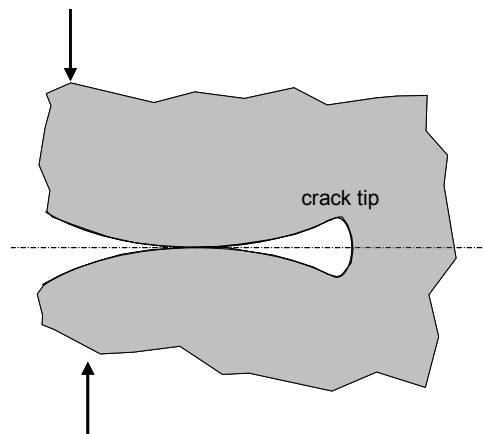


Figure 9 – The mechanism that explains why the crack tip stress intensity factor can increase during a decreasing remote load.

4 Conclusions

An improved Strip Yield model is being developed for the prediction of fatigue crack growth in aluminium components, with particular emphasis on the prediction of crack growth under typical helicopter spectrum loading. The present version of this research model is implemented as a Matlab application, and due to its open and easy architecture it can also serve as a basis to test new concepts that might arise regarding the constraint behaviour of the material at the crack tip, fatigue crack growth propagation laws, etc.

The model has been used to demonstrate that the apparently unique relation between the cyclic crack tip opening displacement, $\Delta CTOD$, and the effective cyclic stress intensity factor, ΔK_{eff} , exists only under the condition of no-crack-closure. Assuming that fatigue crack propagation is driven by cyclic plastic displacements in the crack tip area, it seems worthwhile to further investigate whether the use of $\Delta CTOD$ (possibly in conjunction with $CTOD_{max}$) as the correlating parameter for fatigue crack growth (instead of ΔK_{eff}) will give an improvement in the present capability of the Strip Yield model to predict fatigue crack growth under VA loading.

A possible switch from ΔK_{eff} to $\Delta CTOD$ as the correlating parameter for fatigue crack growth does *not* imply that the vast amount of basic fatigue crack growth data that has been compiled world-wide will become useless: the Strip Yield model can be used as a calibration tool to transform the available experimental da/dN versus ΔK data to da/dN versus $\Delta CTOD$ data.

References

- [1] Dickson, B. Roesch, J., Adams, D. and Krasnowski, B. (1999), “Rotorcraft fatigue and damage tolerance”, Paper 10 in: *Twentyfifth European Rotorcraft Forum*, Rome, Italy.
- [2] Irving, P.E., Lin, J. and Bristow, J.W. (2003), “Damage Tolerance in Helicopters. Report on the Round Robin Challenge”, presented at the *American Helicopter Society 59th Annual Forum*, Phoenix, Arizona, USA.
- [3] Lang, M., Irving, P.E., Stolz, C. and Lin, J. (2005), “Novel robust models for damage tolerant helicopter components”, *Cranfield University Report No: DT 3082Z/66*, approved for public release, Cranfield, UK.
- [4] Zitounis, V. and Irving, P.E. (2007), “Fatigue crack acceleration effects during tensile underloads in 7010 and 8090 aluminium alloys”, *International Journal of Fatigue*, Vol. 29, pp.108-118.
- [5] Vaughan, R.E. and Chang, J.H. (2003), “Life Predictions for High Cycle Dynamic Components Using Damage Tolerance and Small Threshold Cracks”, presented at the *American Helicopter Society 59th Annual Forum*, Phoenix, Arizona, USA.
- [6] Irving, P.E., Zitounis, V. and Buller, R. (2003), “Prediction of Fatigue Crack Growth Rates for Damage Tolerant Helicopter Design - the Role of Load Spectrum and Material”, presented at the *ICCES Conference 2003*, Corfu, Greece.
- [7] Wheeler, O.E. (1972), “Spectrum Loading and Crack Growth”, *Journal of Basic Engineering*, Vol.94, No.1.
- [8] Willenborg, J.; Engle, R.M.; Wood, H.A. (1971), “A Crack Growth Retardation Model Using an Effective Stress Concept”, *Air Force Flight Dynamics Laboratory*, Technical Memorandum TM-71-1-FBR, Dayton, Ohio, USA.
- [9] Wood, H.A. (1973), “A Summary of Crack Growth Prediction Techniques”, AGARD Lecture Series No.62 on Fatigue Life Prediction for Aircraft Structures and Materials, Neuilly-sur-Seine, France.
- [10] Bos, M.J. (1991), “Critical Appraisal of the McDonnell Douglas Closure Model for Predicting Fatigue Crack Growth”, Structures Report 444, *DSTO, Aeronautical Research Laboratory*, Melbourne, Australia.

- [11] Newman, J.C. jr. (1992), "FASTRAN-II – A fatigue crack growth structural analysis program", *NASA Technical Memorandum* 104159 (revised copy), Washington, D.C., USA.
- [12] Fracture mechanics and fatigue crack growth analysis software NASGRO 4.0, Reference Manual, version 4.02, September 2002, *Southwest Research Institute*, San Antonio, Texa, USA.
- [13] Fatigue crack growth computer program "NASGRO" version 3.0, ESACRACK version, Reference Manual (Original Document: JSC-22267B, August 2000); Part of ANNEX 2 to ESACRACK 4 User's Manual (TOS-MCS/2000/41/In, Issue 1).
- [14] Elber, W (1971), "The significance of fatigue crack closure", *Damage Tolerance of Aircraft Structures*, *ASTM STP-486*, American Society for Testing and Materials, pp. 230-242, Philadelphia, PA, USA.
- [15] Dugdale, P.S. (1960), "Yielding of sheets containing slits", *J. of Mech. and Phys. of Solids*, *Vol. 8*.
- [16] Guo, W., Wang, C.H. and Rose, L.R.F. (1999), "The influence of cross-sectional thickness on fatigue crack growth", *Fatigue Fract. Engng. Mater. Struct.*, *Vol. 2*, pp. 437-444.
- [17] Koning, A.U. de, Hoeve, H.J. ten and Henriksen, T.K. (1997), "The description of crack growth on the basis of the Strip Yield model for the computation of crack opening loads, the crack tip stretch and strain rates", *NLR Technical Publication* TP 97511 L, Amsterdam, the Netherlands.
- [18] Carboni, M. (2007), "Strain-gauge compliance measurements near the crack tip for crack closure evaluation: Applicability and accuracy", *Engineering Fracture Mechanics* *Vol. 74*, pp. 563–577.
- [19] Skorupa, M., Machniewicz, T., Skorupa, A., Carboni, M. and Beretta, S. (2002), "Experimental and theoretical investigation of fatigue crack closure in structural steel", *Fatigue 2002*, *Vol. 4/5*, Proceedings of the Eight International Fatigue Congress, Editor A.F. Blom.

- [20] Skorupa, M., Beretta, S., Carboni, M. and Machniewicz, T. (2002), “An algorithm for evaluating crack closure from local compliance measurements”, *Fatigue Fract. Engng. Mater. Struct.*, Vol. 25, pp. 261-273.
- [21] Bos, M.J. (2005), “Guidelines for the use of the Strip Yield model in ESACRACK, WP4 of ESA contract 14923/00/NL/PA on Structural Integrity of Pressurised Structures”, report NLR-CR-2005-295, *National Aerospace Laboratory*, Amsterdam, the Netherlands.
- [22] Kujawski, D. (2005), “On assumptions associated with ΔK_{eff} and their implications on FCG predictions”, *International Journal of Fatigue*, Vol. 27, pp. 1267-1276.
- [23] Sadananda, K. and Vasudevan, A.K. (1997), “Short crack growth behaviour”, *Fatigue and Fracture Mechanics: 27th Volume, ASTM STP 1296*, R.S. Piascik, J.C. Newman, and N.E. Dowling, Eds., American Society for Testing and Materials, pp. 301-316, Philadelphia, PA, USA.
- [24] Wanhill, R.J.H., ‘t Hart, W.G.J., and Schra, L. (1991), “Flight simulation and constant amplitude fatigue crack growth in aluminium-lithium sheet and plate”, *ICAF '91 Tokyo, Aeronautical Fatigue: Key to Safety and Structural Integrity*, A Kobayashi, Ed., Ryoin Co. Ltd. and Eng. Mat. Advisory Services, pp. 393-430.
- [25] Wanhill, R.J.H. and Schra, L. (1990), “Corrosion fatigue crack arrest in aluminum alloys”, *Quantitative Methods in Fractography, ASTM STP 1085*, B.M. Strauss and S.K. Putatunda, Eds., American Society for Testing and Materials, pp. 144-165, Philadelphia, PA, USA.
- [26] Noroozi, A.H., Glinka, G. and Lambert, S. (2005), “A two parameter driving force for fatigue crack growth analysis”, *International Journal of Fatigue*, Vol. 27, pp. 1277-1296.



This page is intentionally left blank.

Appendix A - Crack tip stress/displacement behaviour (graphs)

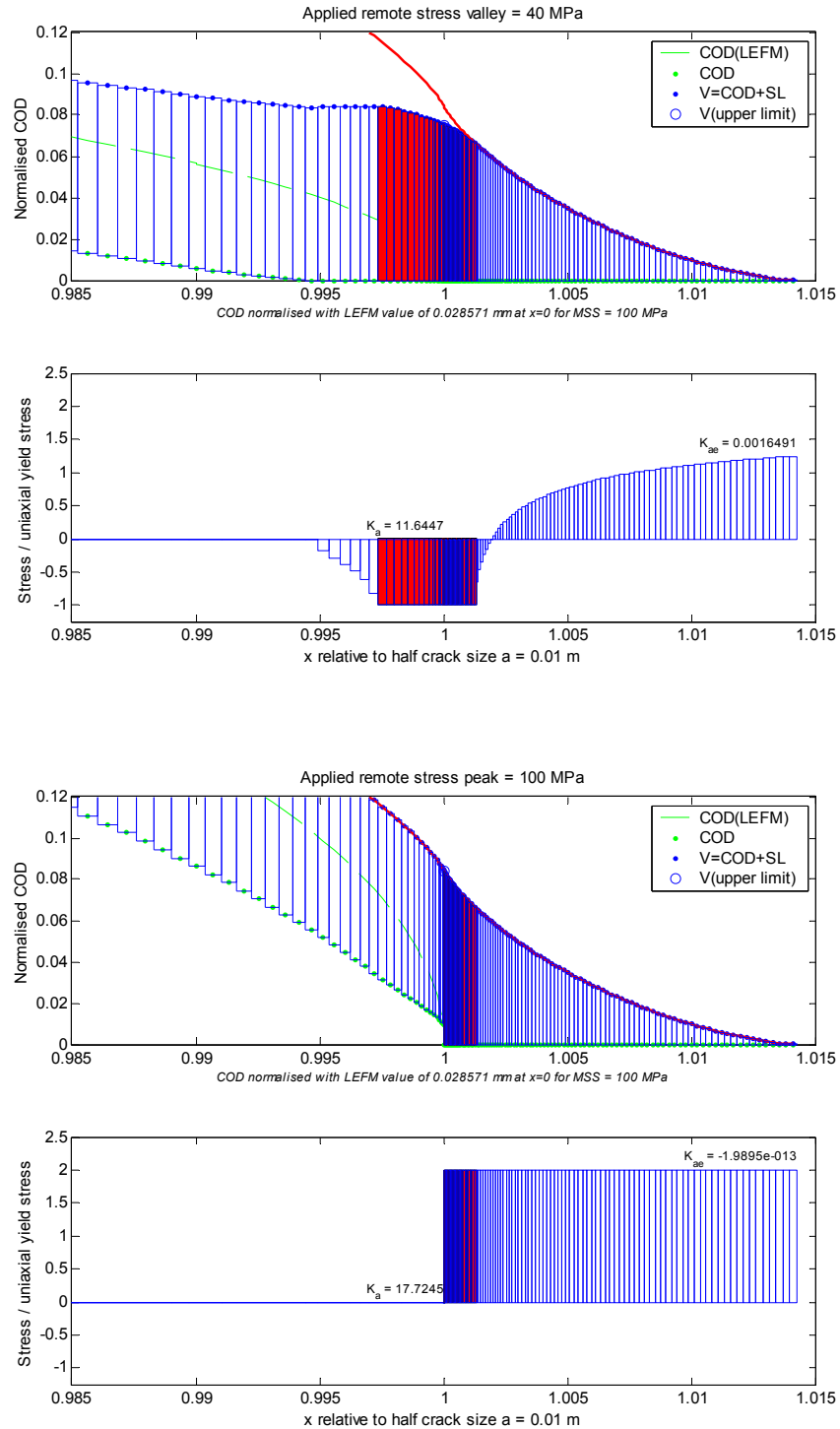


Figure A.1 - Crack opening displacement and local stress around the crack tip, remote stress cycle 40 MPa (top) \rightarrow 100 MPa (bottom); the elements that are yielding are indicated in red.

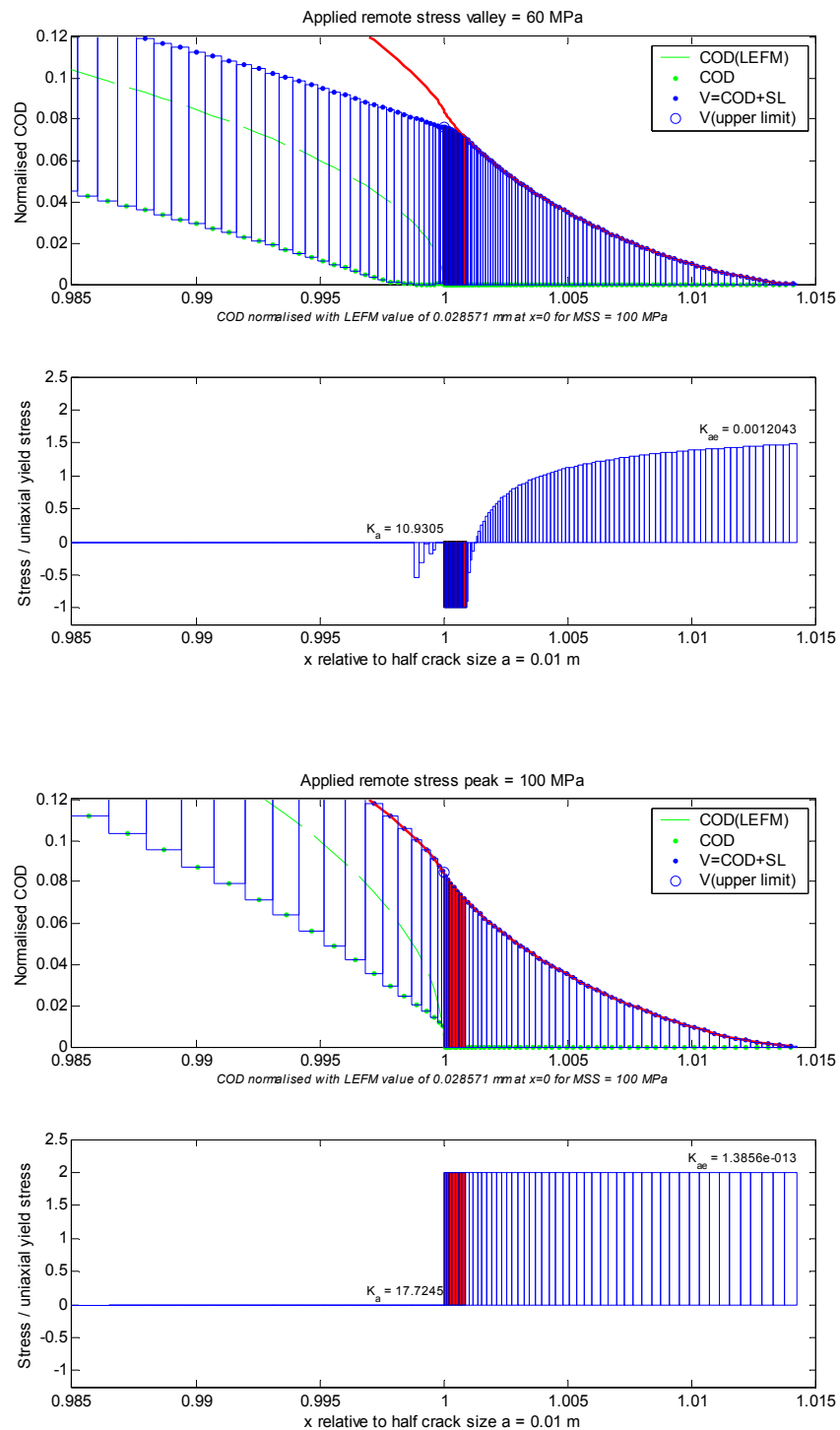


Figure A.2 - Crack opening displacement and local stress around the crack tip, remote stress cycle 60 MPa (top) → 100 MPa (bottom); the elements that are yielding are indicated in red.

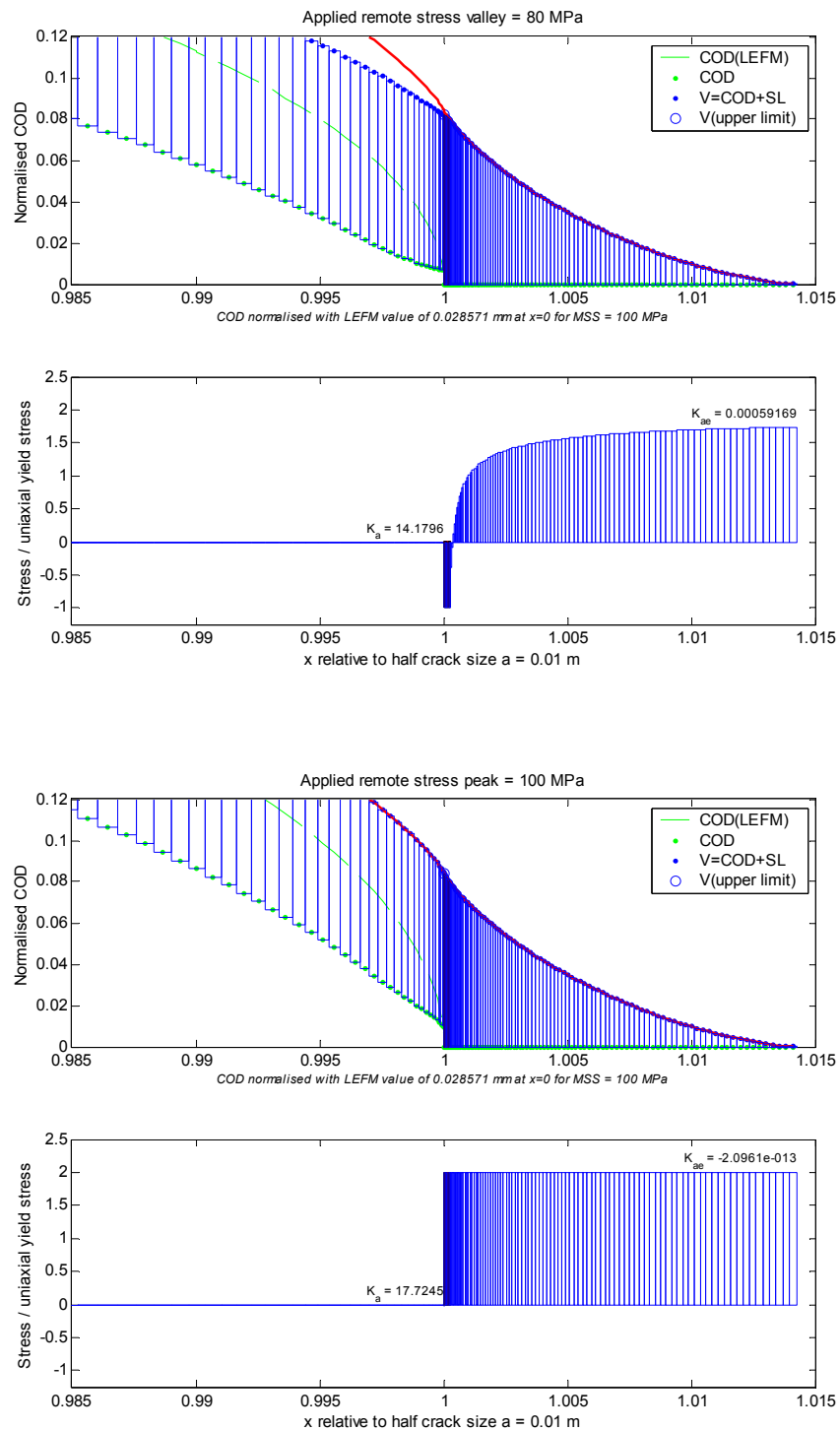


Figure A.3 - Crack opening displacement and local stress around the crack tip, remote stress cycle 80 MPa (top) → 100 MPa (bottom); the elements that are yielding are indicated in red.